Evolution of quantum criticality in $CeNi_{9-x}Cu_xGe_4$

L Peyker[1], C Gold[1], E-W Scheidt[1], W Scherer[1], J G Donath[2], P Gegenwart[3], F Mayr[4], T Unruh[5], V Eyert[6], E Bauer[7] and H Michor[7]

[1] CPM, Institut für Physik, Universität Augsburg, D-86135 Augsburg, Germany
[2] Max Planck Institute for Chemical Physics of Solids, D-01187 Dresden, Germany
[3] I. Physikalisches Institut, Georg-August-Universität, D-37077 Göttingen, Germany
[4] EP V, EKM, Institut für Physik, Universität Augsburg, D-86135 Augsburg, Germany
[5] Forschungsneutronenquelle Heinz Maier-Leibnitz, Technische Universität München, D-85747 Garching, Germany
[6] EP VI, EKM, Institut für Physik, Universität Augsburg, D-86135 Augsburg, Germany
[7] Institut für Festkörperphysik, Technische Universität Wien, A-1040 Wien, Austria

E-mail: Ernst-Wilhelm.Scheidt@physik.uni-augsburg.de and Wolfgang.Scherer@physik.uni-augsburg.de

Abstract

Crystal structure, specific heat, thermal expansion, magnetic susceptibility and electrical resistivity studies of the heavy fermion system $CeNi_{9-x}Cu_xGe_4$ ($0 \leqslant x \leqslant 1$) reveal a continuous tuning of the ground state by Ni/Cu substitution from an effectively fourfold-degenerate non-magnetic Kondo ground state of $CeNi_9Ge_4$ (with pronounced non-Fermi-liquid features) towards a magnetically ordered, effectively twofold-degenerate ground state in $CeNi_8CuGe_4$ with $T_N = 175 \pm 5$ mK. Quantum critical behavior, $C/T \propto \chi \propto -\ln T$, is observed for $x \cong 0.4$. Hitherto, $CeNi_{9-x}Cu_xGe_4$ represents the first system where a substitution-driven quantum phase transition is connected not only with changes of the relative strength of the Kondo effect and RKKY interaction, but also with a reduction of the effective crystal field ground state degeneracy.

(Some figures in this article are in colour only in the electronic version)

1. Introduction

Since the discovery of non-Fermi-liquid (nFL) behavior in $U_{0.2}Y_{0.8}Pd_3$ characterized by a logarithmic divergence of the Sommerfeld coefficient $\gamma \simeq C/T \propto -\ln(T/T_0)$ [1], the research activity in the field of nFL physics has been very active [2]. Therefore, a great deal of attention was devoted to Kondo systems, in particular to those where nFL behavior appears to originate from critical magnetic fluctuations. The latter may emerge near a magnetic phase transition when a subtle balancing of competing interactions shifts a magnetic phase transition towards 0 K. In this quantum critical phase (QCP) scenario [3–5], Kondo interactions, favoring a paramagnetic Fermi-liquid ground state, compete with RKKY interactions, favoring a magnetically ordered ground state (for recent reviews, see [6, 7]).

The relative strength of competing Kondo and RKKY interactions, e.g. in Ce or Yb intermetallics, can be tuned by parameters such as: (i) pressure [8], (ii) substitutions [9] or (iii) external magnetic fields [10]. Besides these tuning parameters controlling the relative strength of Kondo and RKKY interactions, there is another interesting aspect of heavy fermion quantum criticality which was considered in theoretical studies, but hardly explored experimentally, namely the relative magnitudes of Kondo energy and crystal field (CF) level splittings, i.e. the effective number of the total angular momentum degrees of freedom relevant for the Kondo ground state formation. This parameter, abbreviated as *effective spin degeneracy N*, is the number of crystal field states with energies comparable to the Kondo energy or lower. Its variation may also drive a system through a QCP. Coleman [11] has shown that the critical value of the Kondo coupling constant above

which a spin-compensated ground state is stable tends to zero by $1/N$ as N increases, i.e. systems having a large effective spin degeneracy N are less likely to order magnetically.

In this respect, the heavy fermion $CeNi_9Ge_4$ represents a suitable model system to study the role of effective spin degeneracy since it displays larger N values than the usual twofold one in classical nFL systems. Recently, single-ion nFl behavior of the specific heat and magnetic susceptibility has been discussed for this system. Here, $CeNi_9Ge_4$ shows the largest ever recorded value of the electronic specific heat coefficient $\gamma = C/T \approx 5.5$ J K^{-2} mol^{-1} at 0.08 K for paramagnetic Kondo lattices [12, 13]. The dilution of the f moments via Ce/La substitution, i.e. $Ce_{1-y}La_yNi_9Ge_4$, revealed an approximate scaling of the magnetic specific heat contribution and magnetic susceptibility with the cerium ions' fraction, thus indicating that the huge Sommerfeld coefficient γ of $CeNi_9Ge_4$ is mainly due to Ce single-ion effects, i.e. crystal field and Kondo interactions [12]. Another remarkable feature in $CeNi_9Ge_4$ is its strongly temperature-dependent Sommerfeld–Wilson ratio, $R \propto \chi_0/\gamma$, which is revealed by the distinct different temperature dependencies of specific heat and magnetic susceptibility below 1 K [12].

The origin of this behavior is illuminated by $CeNi_9Ge_4$ single-crystal susceptibility and polycrystal magnetic entropy data revealing a crystal field scheme of Ce^{3+} with a quasi-quartet ground state below 20 K. Thereby, a fourfold effective spin degeneracy of the Ce ions is based on two doublets with an energy splitting of only 0.5 meV, i.e. of the same order of magnitude as the Kondo energy in this system, which is about 0.3 meV [14]. Numerical renormalization group (NRG) calculations by Anders and Pruschke [15, 16] using the $SU(4)$ Anderson impurity model which also accounted for crystal field splitting demonstrated that the Kondo effect in combination with a quasi-quartet CF ground state leads to a $SU(2)$ to $SU(4)$ crossover regime with a significant variation of the Sommerfeld–Wilson ratio as experimentally observed in $Ce_{1-y}La_yNi_9Ge_4$.

In this work we study the solid solution $CeNi_{9-x}Cu_xGe_4$, where Ni is gradually replaced by Cu ions up to $x = 1$. This substitution modestly changes the 3d electron number and as a consequence the position of the Fermi level relative to the Ce 4f^1 state. Replacing Ni by Cu is thus expected to influence the Kondo and RKKY interactions. Usually such a substitution should lower the Kondo temperature and support the formation of long range magnetic order. The latter effect is also expected as a consequence of an increasing unit cell volume. Even in the absence of any lattice expansion, Ni/Cu substitution reduces the local point symmetry at Ce sites and thus cancels the quasi-fourfold degeneracy of the CF ground state.

It is important to mention that isostructural and isoelectronic $CeNi_9Si_4$ with an almost 4% smaller unit cell volume exhibits typical Kondo lattice behavior with a Kondo temperature, $T_K \simeq 80$ K [17], being about one order of magnitude larger than T_K of $CeNi_9Ge_4$. X-ray photoelectron spectroscopy on $CeNi_9Si_4$ revealed a cerium valence being close to 3+ ($Ce^{3.0+\delta}$ with $\delta < 0.1$) [18], thus indicating cerium in $CeNi_9Ge_4$ with one order of magnitude lower T_K is $Ce^{3.0+\gamma}$ with $\gamma \ll 0.1$.

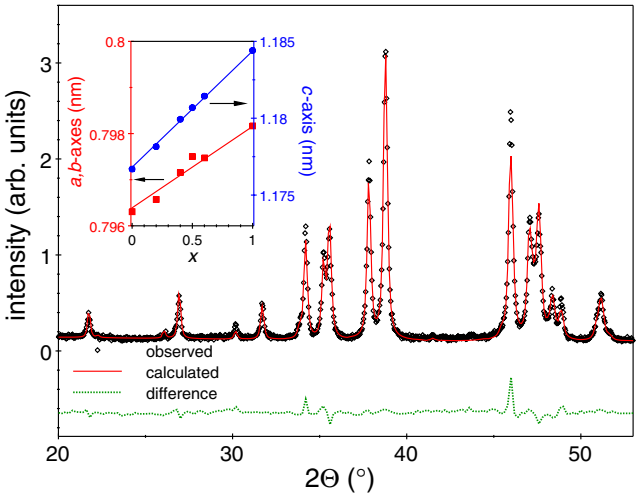

Figure 1. Observed and calculated (Rietveld refinement) x-ray powder diffraction pattern of annealed $CeNi_8CuGe_4$. The dotted line displays the difference plot. The inset shows the variation of the lattice parameters of $CeNi_{9-x}Cu_xGe_4$ with respect to the Cu concentration x.

2. Sample preparation and structural characterization

Polycrystalline samples of $CeNi_{9-x}Cu_xGe_4$ and $LaNi_{9-x}Cu_xGe_4$ were prepared by arc-melting of pure elements, Ce: 4N, La: 3N8 (Ames MPC [19]), Ni: 4N5; Cu: 6N; Ge: 5N, under a highly purified argon atmosphere. To obtain the highest possible homogeneity, the samples were flipped over several times and remelted. Subsequently, the samples were annealed in evacuated quartz-glass tubes for two weeks at 950 °C. Inductively coupled plasma spectroscopy (ICP-OES) studies were carried out and confirmed Ni to Cu ratios in good agreement with the relative amount of the starting materials.

Standard x-ray diffraction techniques using Cu Kα radiation were performed on carefully prepared sieved powdered samples (grain size 40 μm). $CeNi_9Ge_4$ crystallizes in the tetragonal space group $I4/mcm$ with lattice parameters $a = b = 7.9701(1)$ Å and $c = 11.7842(3)$ Å (for structural details, see [12, 13]). From Rietveld analysis (see as one example the $CeNi_8CuGe_4$ pattern in figure 1) precise lattice parameters of the solid solutions were determined. The high quality of the refinement ($R_f = 4.14$) is reflected in the difference plot. The analysis indicates that replacement of the Ni ions by Cu leads to a modest volume expansion, increasing linearly up to 0.8% for $x = 1$ (inset of figure 1). Lattice parameters of $CeNi_8CuGe_4$ are $a = b = 7.9816(7)$ Å and $c = 11.8441(2)$ Å. Total energy calculations based on the new full-potential augmented spherical wave method [20] suggest some degree of preferential occupation of the three inequivalent Wyckoff positions 16k, 16l, and 4d by Cu: $E(16k) < E(4d) < E(16l)$. Indeed, the energy increases for Cu placed on 4d and 16l sites relative to the 16k site are about 0.1 eV and 0.2 eV, respectively.

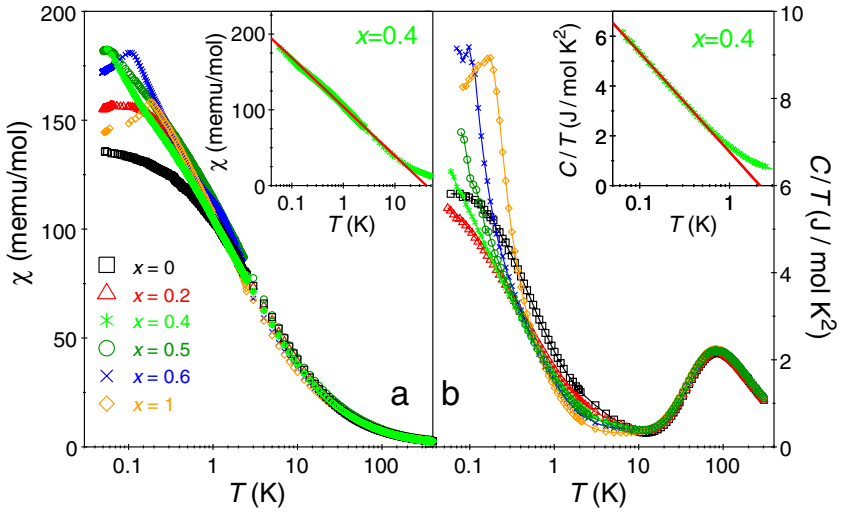

Figure 2. (a) The magnetic susceptibility χ and (b) the specific heat divided by temperature C/T of $CeNi_{9-x}Cu_xGe_4$ in semi-logarithmic plots. AFM transitions are evident for $x \geqslant 0.5$. The insets show χ and C/T versus T of $CeNi_{8.6}Cu_{0.4}Ge_4$: both solid lines represent logarithmic fits over more than one decade in temperature.

3. Experimental results

3.1. Susceptibility and specific heat

The temperature dependence of the dc magnetic susceptibility was measured between 2 and 400 K in an applied magnetic field of 0.5 T with a commercial SQUID magnetometer (MPMS7). In the low temperature region (0.06 K $< T <$ 2.5 K) these measurements were completed by a self-designed ac susceptibility device ($B < 0.3$ mT) installed in a ^{3}He/^{4}He-dilution refrigerator. The absolute values of the low temperature data were obtained by normalizing the ac-χ data to the dc-χ data between 1.8 and 2.5 K. The specific heat experiments were performed with a commercial equipment (PPMS) between 2 and 300 K and in a ^{3}He/^{4}He-dilution refrigerator down to a base temperature (BT) of 60 mK using a standard relaxation method [21].

Figure 2 shows the susceptibility $\chi(T)$ for various compositions of $CeNi_{9-x}Cu_xGe_4$. Above 100 K all samples follow a simple modified Curie–Weiss-type law, $\chi(T) = C/(T - \Theta) + \chi_0$, yielding a paramagnetic Curie–Weiss temperature Θ around -14 K, $\chi_0 \cong 0.9$ memu mol^{-1}, in reasonable agreement with the Pauli susceptibility of $LaNi_9Ge_4$ and a Curie constant C corresponding to an effective paramagnetic moment of $\cong 2.5\ \mu_B$, which is in line with the theoretical value of 2.54 μ_B for a Ce^{3+} ion. Starting from the parent compound $CeNi_9Ge_4$, Ni/Cu substitution initially increases the low temperature susceptibility and reduces the temperature below which it tends to flatten (from $\simeq 1$ K for $x = 0$ to $\simeq 0.2$ K for $x = 0.2$). For $CeNi_{8.6}Cu_{0.4}Ge_4$ we finally observe a $\chi(T) \propto -\ln(T)$ behavior down to the BT of 60 mK (see the inset of figure 2(a)) which is indicative of quantum criticality. At higher Cu concentrations, $x > 0.4$, sharp cusps in $\chi(T)$ indicate phase transitions towards antiferromagnetic (AFM) order. Finally, $CeNi_8CuGe_4$ exhibits magnetic ordering below $T_N \approx 175 \pm 5$ mK.

These observations are corroborated by specific heat results shown as C/T versus T plots for the same compositions of $CeNi_{9-x}Cu_xGe_4$ in figure 2(b). In comparison to $CeNi_9Ge_4$, the initial substitution of Ni by Cu, $x = 0.2$, reduces the C/T values, and the observed deviation from $C/T \propto -\ln(T)$ behavior (which starts below 250 ± 10 mK for $x = 0$) shifts to 150 ± 10 mK. For $CeNi_{8.6}Cu_{0.4}Ge_4$, a $C/T \propto -\ln(T)$ divergence of the Sommerfeld coefficient holds over more than one decade in temperature down to the BT of 60 mK (see the inset of figure 2(b)). We note that, despite the common $-\ln(T)$ behavior of specific heat and susceptibility of $CeNi_{8.6}Cu_{0.4}Ge_4$, a simple proportionality $\chi \propto C/T$ is not observed. Rather, these quantities reveal a temperature-dependent Sommerfeld–Wilson ratio, $R \propto \chi_0/\gamma$, which has been discussed in terms of CF effects in the case of $CeNi_9Ge_4$ [15, 16]. Above $x = 0.4$, magnetic phase transitions are clearly indicated by specific heat anomalies superimposed on a huge background due to heavy electrons with Sommerfeld values C/T exceeding 9 J mol^{-1} K^{-2} for $CeNi_{8.4}Cu_{0.6}Ge_4$.

To check whether the nature of magnetic ordering of $CeNi_8CuGe_4$ is long range AFM or of spin-glass type, we performed low temperature ac susceptibility measurements for two different frequencies (95 and 995 Hz) which are shown in figure 3. The absence of any significant frequency dependence of the sharp cusp of $\chi'_{ac}(T)$ rules out a spin-glass type of magnetic transition. Rather, it is a strong hint towards long range AFM order (compare, for example, [22]). The AFM nature of the magnetic transition in $CeNi_8CuGe_4$ is further supported by local probe muon spin relaxation (μSR) studies which will be published elsewhere [23]. μSR signals compatible with the spin-glass or cluster-glass type of magnetism have not been observed for $CeNi_8CuGe_4$ nor for $CeNi_{8.6}Cu_{0.4}Ge_4$ or $CeNi_9Ge_4$ for measurements down to 40 mK.

3.2. Volume thermal expansion

The volume thermal expansion $\alpha(T) = 1/V(\partial V/\partial T)$ is ideally suited to study nFL behavior that results from a

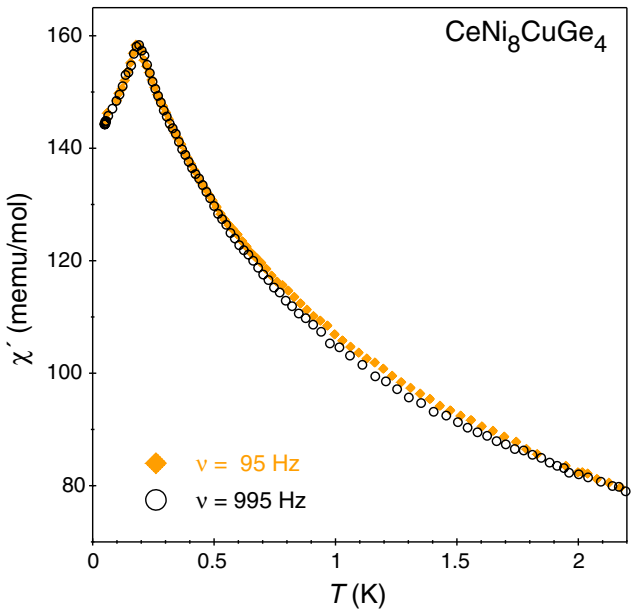

Figure 3. The ac susceptibility χ' of $CeNi_8CuGe_4$ is plotted linear over T for two frequencies (closed diamonds: 95 Hz and open circles: 995 Hz).

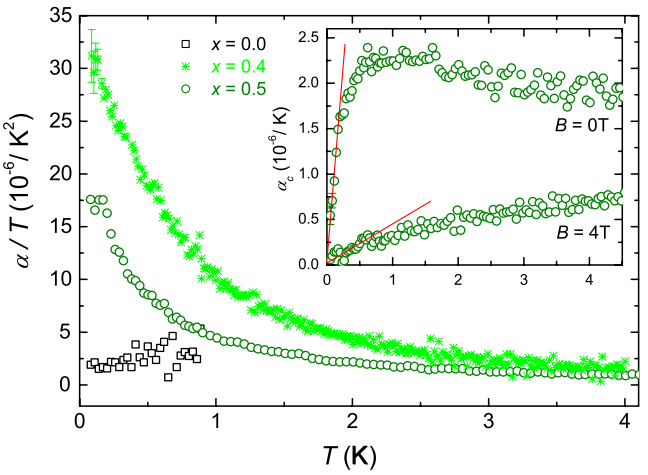

Figure 4. Volume thermal expansion coefficient $\alpha(T)/T$ versus T of $CeNi_{9-x}Cu_xGe_4$ for $x = 0$, 0.4 and 0.5. The errors are indicated by vertical bars. Inset: linear thermal expansion coefficient $\alpha_c(T)$ of $CeNi_{8.5}Cu_{0.5}Ge_4$ for $B = 0$ and 4 T. Lines represent fits $\alpha_c(T) = a_1\,T$ with $a_1 = 9 \times 10^{-6}$ K^{-2} and $a_1 = 4 \times 10^{-7}$ K^{-2} for $B = 0$ T and $B = 4$ T, respectively.

QCP, because $\alpha(T) \propto (\partial S/\partial p)$ directly probes the pressure dependence of the entropy which is accumulated close to the instability. A theoretical study in terms of a scaling analysis suggested that the thermal expansion is far more singular than the specific heat $C(T)/T$ at any pressure-sensitive QCP [24].

We obtained $\alpha(T)$ by means of a high-resolution capacitive dilatometer (redesigned after Pott and Schefzyik [25]) attached to a ^{3}He/^{4}He-dilution refrigerator. Measurements on selected compositions $CeNi_{9-x}Cu_xGe_4$ with $x = 0, 0.4$ and 0.5 were carried out between 0.08 K $< T <$ 4 K and in applied magnetic fields up to 4 T. The volume thermal expansion α is given by the sum of the linear thermal expansion coefficients along three perpendicular directions a, b and c, i.e. $\alpha = \alpha_a + \alpha_b + \alpha_c$. Assuming isotropic behavior in our polycrystalline samples, we have obtained the volume expansion as $\alpha = 3\alpha_a$. For the data in a magnetic field, the linear expansion coefficient along the direction of the applied magnetic field has been determined and denoted as α_c in the following. This estimate does not take into account that texture may play a role in particular for $CeNi_9Ge_4$.

Figure 4 shows the volume thermal expansion $\alpha(T)/T$ versus T for various concentrations $x = 0, 0.4$ and 0.5 for $CeNi_{9-x}Cu_xGe_4$. It reaches remarkably high values of the order of 10^{-6} K^{-2}, typical for heavy fermion compounds. In agreement with the susceptibility data of the undoped sample, we find $\alpha(T)/T =$ constant for $T < 1$ K, indicative for an FL ground state. Substituting Cu for Ni generates singular behavior in $\alpha(T)/T$ which is most pronounced for $x = 0.4$. Further increasing the Cu content causes a saturation of $\alpha(T)/T$ at lowest temperatures $T < 0.2$ K for $x = 0.5$. A suppression of the critical fluctuation is also observed by applying a magnetic field, which is demonstrated for $CeNi_{8.5}Cu_{0.5}Ge_4$ in the inset of figure 4. While for $B = 0$ T, FL behavior, i.e. $\alpha_c(T)/T =$ const. is found only up to $T \approx 0.2$ K, this behavior extends until $T \approx 0.8$ K for $B = 4$ T. At the same time, the linear coefficient a_1 of the FL contribution to the thermal expansion coefficient $\alpha_c(T) \simeq a_1 T$ varies by an order of magnitude from $a_1(B = 0\ \mathrm{T}) = 9 \times 10^{-6}$ K^{-2} to $a_1(B = 4\ \mathrm{T}) = 4 \times 10^{-7}$ K^{-2}, indicating that α_c/T is strongly suppressed in a magnetic field. Such behavior is found in many quantum critical systems [26, 27].

3.3. Electrical resistivity

The concentration-dependent crossover from Kondo lattice behavior with unusual single-ion nFl features of the specific heat and magnetic susceptibility in $CeNi_9Ge_4$ to long range magnetic order in $CeNi_{9-x}Cu_xGe_4$ is also revealed by resistivity measurements (figure 5(a)). While the $LaNi_9Ge_4$ reference sample exhibits a normal metallic Bloch–Grüneisen behavior with a very low residual resistivity of 5 $\mu\Omega$ cm, $CeNi_9Ge_4$ seems to represent a classical Kondo lattice, with a residual resistivity $\rho_0 \simeq 9$ $\mu\Omega$ cm of a very pure sample. After passing a minimum around 30 K and a logarithmic increase, the resistivity follows a $1 - T^2$ law, as is known for Kondo systems. At lower temperatures the resistivity passes through a maximum at a temperature $T^* \simeq 3$ K and follows a T^2-behavior below the Fermi liquid temperature $T_{\mathrm{FL}} = 160 \pm 20$ mK. While T_{FL} is close to the temperature where C/T deviates from the $C/T \propto -\ln T$ trend, T^* coincides approximately with the temperature below which the susceptibility of $CeNi_9Ge_4$ deviates from the $\chi \propto -\ln T$ behavior of $CeNi_{8.6}Cu_{0.4}Ge_4$.

The drastic initial rise of the residual resistivity between $x = 0$ and 0.2 is also observed in the solid solution $CeNi_9Ge_{4-x}Si_x$ for $x < 0.1$ [28]. This increase seems to be related to the reduction of the local site symmetry of the cerium ions which again leads to modified crystal field effects and Kondo coherence. In the same concentration range the corresponding $LaNi_9Ge_{4-x}Si_x$ series simply follows the

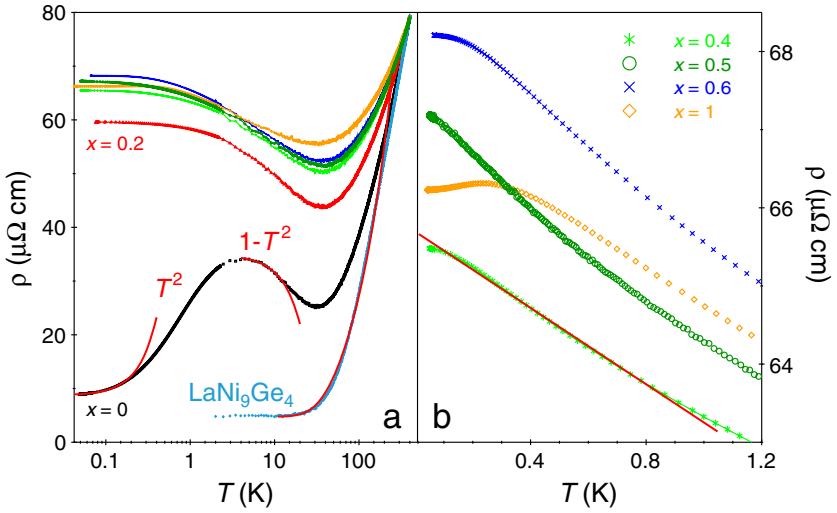

Figure 5. (a) A semi-logarithmic plot of the electrical resistivity $\rho(T)$ of $CeNi_{9-x}Cu_xGe_4$ normalized at 300 K to that of $LaNi_9Ge_4$ which was measured with the Van der Pauw method. The solid lines depict T^2 fits for $CeNi_9Ge_4$ and a Bloch–Grüneisen fit for $LaNi_9Ge_4$. $CeNi_9Ge_4$ exhibits Kondo lattice behavior. (b) In a linear plot of ρ versus T the development of a long range ordered AFM phase transition is observed for $x \geqslant 0.5$, while the resistivity for $CeNi_{8.6}Cu_{0.4}Ge_4$ is linear down to 80 mK (solid line).

Nordheim law [29] describing the variation of the residual resistivity upon substitutional disorder.

For the Cu substituted samples the resistivity $\rho(T)$ passes through a Kondo minimum around 30 K, followed by a logarithmic increase at lower temperatures. For $x = 0.4$ the resistivity increases linearly below 1 K, indicating nFL behavior (figure 5(b)). This particular behavior was observed for so-called disordered Kondo systems [30, 31]. For $x \geqslant 0.5$ the resistivity exhibits a bending at lower T for some samples and a maximum for $CeNi_8CuGe_4$ denoting long range magnetic order. This is in line with the evolution of the AFM transition observed in C/T and χ measurements.

4. Discussion

4.1. Analysis of the high temperature specific heat

To track the mechanism driving the system from Kondo lattice behavior with unusual nFL features towards RKKY antiferromagnetism, we extract the magnetic contribution of the specific heat by subtracting the total specific heat of the system $LaNi_{9-x}Cu_xGe_4$ with unoccupied 4f states. We therefore synthesized the $4f^0$ reference compounds $LaNi_9Ge_4$ and $LaNi_8CuGe_4$ and interpolated the total specific heat data of the corresponding La sample for each respective composition linearly.

The magnetic contribution to the specific heat ΔC of all $CeNi_{9-x}Cu_xGe_4$ samples is depicted in figure 6. The reliability of ΔC is indicated by vertical error bars which become larger at high temperature because of the relatively large phonon background. For $CeNi_9Ge_4$, two pronounced maxima occur around 5 and 35 K. The former is associated with the effectively fourfold-degenerate Kondo lattice ground state which is composed by $\Gamma_7^{(1)}$ and $\Gamma_7^{(2)}$ CF doublets with an energy splitting of comparable magnitude as the Kondo energy [15, 16]. Thus, a broad Kondo-like contribution rather

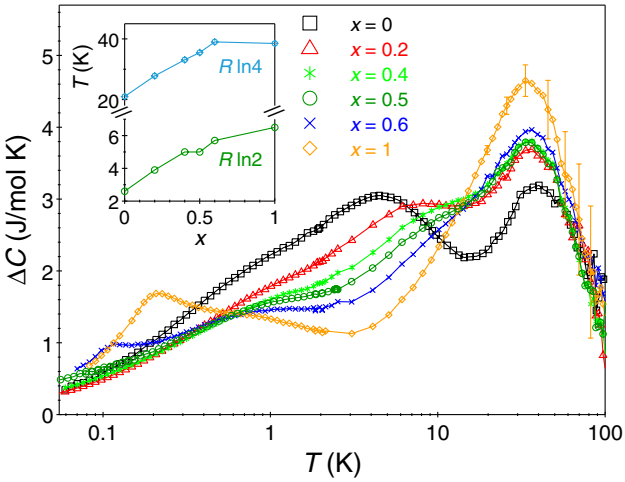

Figure 6. Temperature dependence of the magnetic specific heat ΔC of $CeNi_{9-x}Cu_xGe_4$ in semi-logarithmic representation. The errors are indicated by vertical bars exemplary for $CeNi_8CuGe_4$. The resulting temperatures where the entropy reaches $R \ln 2$ and $R \ln 4$ with respect to the Cu concentration x are plotted in the inset.

than a CF Schottky anomaly becomes visible. The second Schottky-like maximum at about 35 K is associated with a third CF doublet (Γ_6). With increasing Cu concentration this specific heat maximum gains in height, but remains roughly at the same position near 35 K. In contrast, the lower Kondo-like maximum decreases and broadens. At a Cu concentration of $x = 0.4$ a clear separation is observed dividing the broad hump into a low lying anomaly around 0.8 K, while the upper anomaly is shifted towards higher temperature. Finally, for $x = 1$, the latter merges with the Schottky contribution centered at about 35 K. The appearance of two separated maxima upon Ni/Cu substitution, originating from the initially single but broad low temperature maximum of pure $CeNi_9Ge_4$, indicates a reduction of the effective spin degeneracy of the Ce

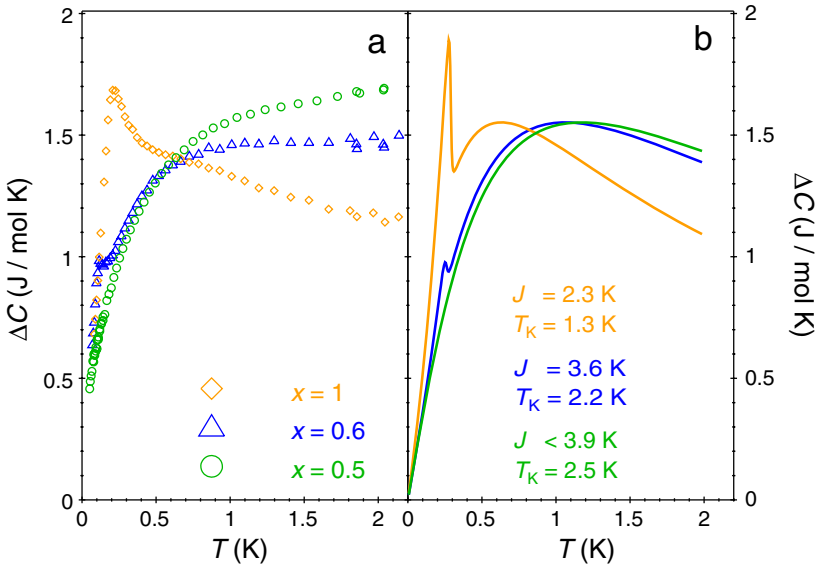

Figure 7. (a) Magnetic contribution to the temperature-dependent specific heat ΔC of $CeNi_{9-x}Cu_xGe_4$ plotted versus T below 2 K. (b) Model calculations for the specific heat according to the resonant-level model of Schotte and Schotte [32] (see text).

ions from fourfold in the case of $CeNi_9Ge_4$ to a twofold one for $CeNi_{8.6}Cu_{0.4}Ge_4$.

The evolution of the temperature-dependent magnetic entropy gain, $\Delta S(T)$, further supports a change of energy scales. The inset in figure 6 shows those temperatures where the entropy approaches $R\ln 2$ and $R\ln 4$ in dependence on the Cu concentration. Both values, $T(S = R\ln 2)$ and $T(S = R\ln 4)$, increase significantly from $CeNi_9Ge_4$ to $CeNi_{8.4}Cu_{0.6}Ge_4$, thus indicating a distinct change of the CF scheme and/or Kondo energy scale. An increase of the Kondo energy may be anticipated from the observed increase of $T(S = R\ln 2)$, but this trend contradicts the expectation of the change in electron number and unit cell volume, namely a reduction of T_K when proceeding from $CeNi_9Ge_4$ to $CeNi_8CuGe_4$.

4.2. Discussion of the low temperature specific heat

To obtain a more reliable estimate for the trend of the Kondo energies in $CeNi_{9-x}Cu_xGe_4$ we utilized the resonant-level model by Schotte and Schotte [32] in combination with a molecular field approach to account for long range magnetic order [33, 34].

For a spin-1/2 system the magnetic contribution of the specific heat $C_{mag}(T)$ follows in this model from

$$C_{mag} = 2k_B\,\mathrm{Re}\left\{\frac{z}{T}\left[1-\left(\frac{z}{T}-\frac{\partial z}{\partial T}\right)\psi'\left(\frac{1}{2}-\frac{z}{T}\right)\right]\right\}, \quad (1)$$

where $z = T_K + iE(T)/2\pi k_B$, with T_K the Kondo temperature, E the Zeeman energy and ψ' the derivative of the digamma function. By factoring the mean-field theory into the resonant-level model, E gets temperature-dependent with

$$E(T) = g\mu_B\lambda M(T) = J\frac{M(T)}{g\mu_B}. \quad (2)$$

Here g is the Landé factor (for Ce^{3+}: $g = 6/7$), λ is the molecular field constant, J describes the s–f exchange interaction and $M(T)$ is the simple magnetization for a two-level system. Since the levels are broadened by the Kondo effect the simple Brillouin function becomes modified and $M(T)$ is

$$M(T) = \frac{g\mu_B}{\pi}\,\mathrm{Im}\left[\psi\left(\frac{1}{2}+\frac{T_K + iE(T)}{2\pi k_B T}\right)\right]. \quad (3)$$

Finally, while equations (2) and (3) are implicit equations for $E(T)$ and $M(T)$, respectively, we have to calculate the specific heat (equation (1)) numerically.

Model calculations for specific heat data were done for all samples with $x \geqslant 0.5$. In this composition range, $T(S = R\ln 2)$ and $T(S = R\ln 4)$ are roughly constant at values almost twice as large as for $CeNi_9Ge_4$ (inset of figure 6).

The results are plotted in figure 7. The simple molecular field model plus the Kondo effect within a doublet ground state, of course, does not account for any kind of short range magnetic correlations or fluctuations. Therefore it cannot be taken into account for the experimental data over an extended temperature range. Nevertheless, it qualitatively reproduces the evolution of the magnetic specific heat anomalies and Kondo contributions of $CeNi_{9-x}Cu_xGe_4$ for $x > 0.5$. The exchange interactions J and the Kondo temperatures T_K obtained from the resonant-level model are recorded in figure 7(b). In addition, T_K is depicted in a magnetic phase diagram of $CeNi_{9-x}Cu_xGe_4$ (see section 4.4). A linear extrapolation of the T_K values above $x = 0.5$ results in a $T_K = 3.5$ K for $CeNi_9Ge_4$, which is in line with T_K revealed by the quasi-elastic linewidth observed by quasi-elastic neutron scattering [14]. The substantial reduction of T_K with increasing Cu concentration is in accordance with the usual trend observed in the case of Ni/Cu substitution in other cerium heavy fermion systems [35]. In addition, the drop of

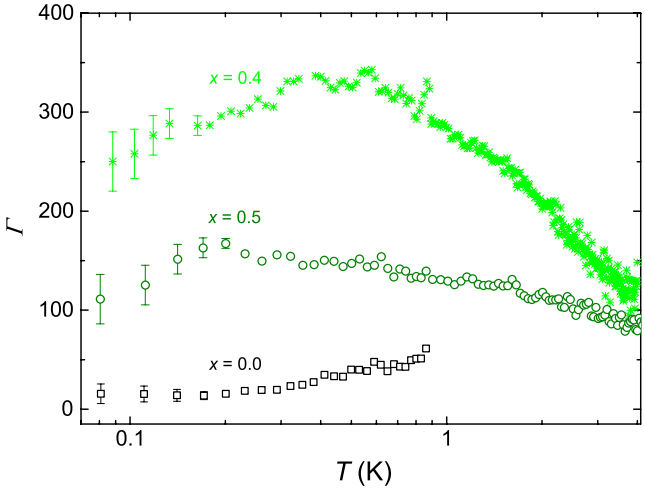

Figure 8. Temperature dependence of the dimensionless Grüneisen ratio $\Gamma(T) = V_m/\kappa_T\alpha(T)/C(T)$ of $CeNi_{9-x}Cu_xGe_4$ in semi-logarithmic representation ($V_m = 7.485 \times 10^{-28}$ m^3, $\kappa_T = 1 \times 10^{-11}$ Pa^{-1}, see text for details).

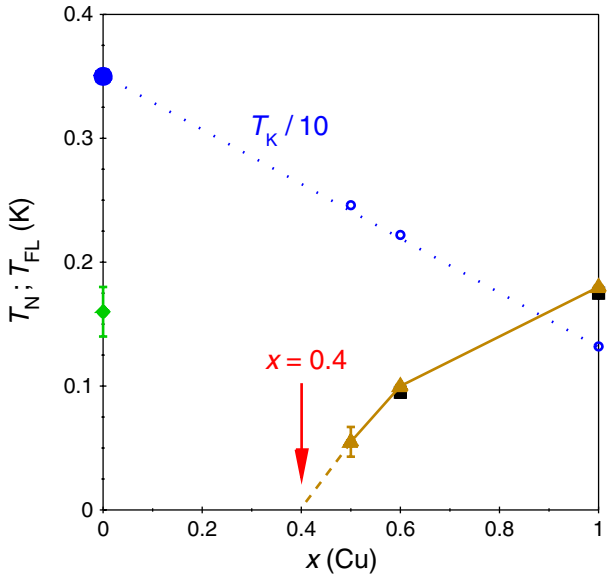

Figure 9. Magnetic phase diagram of $CeNi_{9-x}Cu_xGe_4$: the squares and triangles depict T_N as extracted from the C/T and χ data, respectively, while the diamond represents T_{FL} derived from ρ. The Kondo temperature T_K (full circle) for $x = 0$ is revealed by the quasi-elastic linewidth observed by inelastic neutron scattering studies [14]. For $x \geqslant 0.5$ (open circles) T_K is roughly estimated from comparison with model calculations in terms of the resonant-level model of Schotte and Schotte [32] (see figure 7(b)).

T_K combined with the lowering of the exchange interaction parameter J is in agreement with the Doniach picture [36]. Therefore, the change of the magnetic entropy gain observed from $x = 0$ to 0.5 is attributed to CF effects causing a reduction of the effective spin degeneracy of Ce ions from fourfold in the case of $CeNi_9Ge_4$ to a twofold one for $CeNi_{8.6}Cu_{0.4}Ge_4$.

4.3. Thermal expansion and Grüneisen ratio

To analyze the nature of the QCP indicated by the thermodynamic data of $CeNi_{8.6}Cu_{0.4}Ge_4$ we calculate the dimensionless Grüneisen ratio $\Gamma(T) = (V_m/\kappa_T)\times\alpha(T)/C(T)$ displayed in figure 8 for $CeNi_{9-x}Cu_xGe_4$ with $x = 0$, 0.4 and 0.5. In this calculation of $\Gamma(T)$, the molar volume is $V_m = 7.485 \times 10^{-28}$ m^3 and the isothermal compressibility is assumed to be $\kappa_T = 1 \times 10^{-11}$ Pa^{-1}, which is a typical value for heavy fermion systems. The temperature-independent Grüneisen ratio of $CeNi_9Ge_4$ [$\Gamma(T) = $ const.] below 200 mK and the enhanced values of Γ compared to the usual metals characterize $CeNi_9Ge_4$ as a Kondo lattice system [37]. In contrast to the latter system, both $CeNi_{8.6}Cu_{0.4}Ge_4$ and $CeNi_{8.5}Cu_{0.5}Ge_4$ exhibit an order of magnitude higher Γ value which is typical for heavy fermion systems close to a magnetic instability [26, 38, 39]. For the antiferromagnetic system $CeNi_{8.5}Cu_{0.5}Ge_4$, a negative Grüneisen ratio is expected below the Néel temperature ($T_N = 55$ mK). The decrease of $\Gamma(T)$ below 0.2 K may indicate short range order above T_N. In particular for $CeNi_{8.6}Cu_{0.4}Ge_4$ the high Γ values [$\Gamma(0.35\text{ K}) = 340$] and the strong temperature dependence of $\Gamma(T)$ above 0.35 K are quite different to the parent compound $CeNi_9Ge_4$ and suggest the vicinity of a QCP. Below 0.35 K, $\Gamma(T)$ saturates and passes a broad maximum, indicating that quantum critical behavior, i.e. the divergence of $\Gamma(T \rightarrow 0)$ suggested by Zhu *et al* [24], is vanishing at very low temperatures. This could be explained by assuming that either the $x = 0.4$ system is located somewhat away from the QCP or that the quantum phase transition is slightly rounded by disorder in line with the results of the electrical resistivity. Above 0.35 K the Grüneisen ratio follows, within experimental resolution, a logarithmic dependence, which clearly deviates from the scaling prediction for a standard QCP by Zhu *et al* [24]. We speculate that the reduction of the effective crystal field ground state degeneracy near the quantum phase transition may modify quantum criticality in our system.

4.4. Evolution of quantum criticality and crystal field

The phase diagram of $CeNi_{9-x}Cu_xGe_4$ illustrates the presence of a quantum phase transition near $x = 0.4$ (figure 9). The FL temperature T_{FL} of $CeNi_9Ge_4$ is estimated from the deviation from T^2 behavior of the resistivity at low temperature (see figure 5). In addition, the Néel temperature T_N is derived from the sharp kink of C/T and the susceptibility found in the AFM region. At the critical composition, $CeNi_{8.6}Cu_{0.4}Ge_4$, C/T and $\chi(T)$ display a logarithmic temperature dependence over more than one decade in temperature at least down to 60 mK and the thermal expansion coefficient α/T diverges. These results signify the presence of a heavy fermion QCP. In $CeNi_{8.6}Cu_{0.4}Ge_4$, the nFL state develops from a crossover between a Kondo state ($x \leqslant 0.4$) to an antiferromagnetic coherent state ($x \geqslant 0.4$) starting from $T_N = 0$ K at $x \simeq 0.4$. The question arises whether this crossover is mainly driven by 'disorder' in the energy phase space (originated by substitutional disorder) or mainly by the reduction of the effective ground state degeneracy in combination with a reduction of the Kondo energy. The latter scenario implies that the crossover from the paramagnetic to the AFM ground

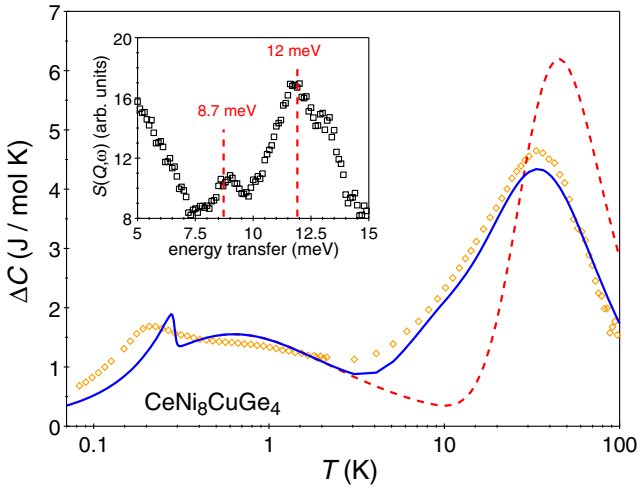

Figure 10. The magnetic contribution of the specific heat ΔC of $CeNi_8CuGe_4$ is plotted from 70 mK to 100 K. The dashed and solid lines are theoretical adjustments to the data taking into account the resonant-level model [32] and two Schottky terms originating from only one (dashed line) or two (solid line) different CF environments, respectively (see text). The inset shows the energy-loss spectra of an inelastic neutron scattering experiment taken at 4 K with $\lambda = 2.2$ Å (instrumental resolution: 1.0 meV full width at half-maximum of the elastic line).

state is connected with a QCP similar to the one discussed for $CeCu_{6-x}Au_x$ [40].

To elucidate the change of the CF scheme in the solid solution from $CeNi_9Ge_4$ with a quasi-fourfold ground state [12, 14] to $CeNi_8CuGe_4$ we have quantitatively analyzed the magnetic contribution to the specific heat ΔC of $CeNi_8CuGe_4$ by model calculations combining specific CF schemes with an energy-split ground state doublet as considered above in the resonant-level model for $CeNi_8CuGe_4$ with $J = 2.3$ K and $T_K = 1.3$ K (see figure 7(b)). The bases for these calculations are preliminary inelastic neutron scattering (INS) data, where two crystal field transitions at 8.7 meV (≈101 K) and 12.0 meV (≈139 K) were obtained from energy-loss spectra (inset, figure 10). In figure 10 two model cases considering different crystal field tuning mechanisms are displayed. The first one is based on a unique crystal field environment for each cerium atom using the CF level extracted from the INS experiment. Here the CF splitting of the $j = 5/2$ state, $\Delta_1 = 101$ K, is significantly larger than $\Delta_1 \sim 6$ K of the undoped $CeNi_9Ge_4$, whereas $\Delta_2 = 139$ K is of similar magnitude [14] (see the dashed line in figure 10). The second model scenario considers two or more different CF environments arising from a stochastic occupation of the Cu atoms on the Ni1 site (Wyckoff position 16k; section 2). For example, the solid line in figure 10 represents a model calculation based on two weighted CF schemes consisting of $\Delta_1 = 26$ K, $\Delta_2 = 101$ K (40%) and $\Delta_1 = 71$ K, $\Delta_2 = 139$ K (60%). Here the two CF transitions from the INS studies were utilized to describe each upper CF level Δ_2 of the two different environments. The latter model is in better agreement with the experimental specific heat data of $CeNi_8CuGe_4$, thus indicating some variability of the local CF level schemes due to substitutional disorder, but nevertheless, relatively defined excitation energies and a twofold degenerate CF ground state. The model (solid line in figure 10) with a doublet ground state split by molecular field and Kondo effect and finite excitation energies, $\Delta \geqslant 26$ K, to further CF doublets accounts rather well for the overall entropy gain revealed by the magnetic contribution to the specific heat. It confirms that the increase of $T(S = R \ln 2)$ in the solid solution $CeNi_{9-x}Cu_xGe_4$ displayed in the inset of figure 6 is the consequence of the change of the CF ground state from effectively fourfold- to twofold-degenerate. Therefore, the trend of $T(S = R \ln 2)$ upon Ni/Cu substitution is not inconsistent with a reduction of the Kondo temperature T_K which is expected from the lattice expansion in $CeNi_{9-x}Cu_xGe_4$ and also indicated by the comparison with model calculations displayed in figure 7.

The nFL behavior of $CeNi_{8.6}Cu_{0.4}Ge_4$ is thus attributed to a QCP caused by a reduction of the Kondo temperature in combination with a disorder-induced reduction of the local site symmetry of cerium ions which alters the effective ground state degeneracy. While the Kondo disorder model considers a Kondo singlet ground state with varying local coupling strength, a different aspect is more relevant in the present case, namely the reduction of the local site symmetry of cerium ions which changes the local ground state from effectively fourfold- to twofold-degenerate. Such symmetry changes would generally be expected to be very susceptible to disorder: as we have seen above, this kind of scenario could consistently explain our experimental results.

5. Summary

In conclusion, in the system $CeNi_{9-x}Cu_xGe_4$ ($0 \leqslant x \leqslant 1$) the change from an effectively fourfold-degenerate to a twofold-degenerate ground state is accompanied by a quantum phase transition near $CeNi_{8.6}Cu_{0.4}Ge_4$ which separates $CeNi_9Ge_4$, a Kondo lattice with unusual nFL features, from the antiferromagnetically ordered state for $x \geqslant 0.4$. In this solid solution Ni/Cu substitution crucially alters the local CF environment of the Ce ions. This leads to a quantum phase transition, which is not only driven by the competition between the Kondo effect and RKKY interaction, but also by a reduction of the effective CF ground state degeneracy.

Acknowledgments

We acknowledge valuable discussions with S Kehrein. This work was supported by the Deutsche Forschungsgemeinschaft (DFG) under contract no. SCHE487/7-1 and research unit 960 'Quantum phase transitions' by the COST P16 ECOM Project of the European Union.

References

[1] Seaman C L, Maple M B, Lee B W, Ghamaty S, Torikachvili M S, Kang J-S, Liu L Z, Allen J W and Cox L D 1991 *Phys. Rev. Lett.* **67** 2882
[2] Stewart G R 2001 *Rev. Mod. Phys.* **73** 797
Stewart G R 2006 *Rev. Mod. Phys.* **78** 743

[3] Hertz J A 1976 *Phys. Rev.* B **14** 1165
[4] Millis A J 1993 *Phys. Rev.* B **48** 7183
[5] Moriya T and Takimoto T 1995 *J. Phys. Soc. Japan* **64** 960
[6] von Löhneysen H, Rosch A, Vojta M and Wölfle P 2007 *Rev. Mod. Phys.* **79** 1015
[7] Gegenwart P, Si Q and Steglich F 2008 *Nat. Phys.* **4** 186
[8] Bogenberger B and von Löhneysen H 1995 *Phys. Rev. Lett.* **74** 1016
[9] Andraka B and Stewart G R 1993 *Phys. Rev.* B **47** 3208
[10] Heuser K, Scheidt E-W, Schreiner T and Stewart G R 1998 *Phys. Rev.* B **57** R4198
[11] Coleman P 1983 *Phys. Rev.* B **28** 5255
[12] Killer U, Scheidt E-W, Eickerling G, Michor H, Sereni J, Pruschke T and Kehrein S 2004 *Phys. Rev. Lett.* **93** 216404
[13] Michor H, Bauer E, Dusek C, Hilscher G, Rogl P, Chevalier B, Etourneau J, Giester G, Killer U and Scheidt E-W 2004 *J. Magn. Magn. Mater.* **272–276** 227
[14] Michor H *et al* 2006 *Physica* B **378–380** 640
[15] Scheidt E-W, Mayr F, Killer U, Scherer W, Michor H, Bauer E, Kehrein S, Pruschke T and Anders F 2006 *Physica* B **378–380** 154
[16] Anders F and Pruschke T 2006 *Phys. Rev. Lett.* **96** 086404
[17] Michor H, Berger S, El-Hagary M, Paul C, Bauer E, Hilscher G, Rogl P and Giester G 2003 *Phys. Rev.* B **67** 224428
[18] Wang X, Michor H and Grioni M 2007 *Phys. Rev.* B **75** 035127
[19] Materials Preparation Center, Ames Laboratory, US DOE Basic Energy Sciences, Ames, IA, USA available from: www.mpc.ameslab.gov
[20] Eyert V 2007 *The Augmented Spherical Wave Method—A Comprehensive Treatment* (*Lecture Notes in Physics* vol 719) (Berlin: Springer)
[21] Bachmann R *et al* 1972 *Rev. Sci. Instrum.* **43** 205
[22] Körner S, Weber A, Hemberger J, Scheidt E-W and Stewart G R 2000 *J. Low Temp. Phys.* **121** 105
[23] Michor H and Hillier A D 2006 *ISIS Experimental Report* RB520265 unpublished
[24] Zhu L, Garst M, Rosch A and Si Q 2003 *Phys. Rev. Lett.* **91** 066404
[25] Pott R and Schefzyik R 1983 *J. Phys. E: Sci. Instrum.* **16** 444
[26] Küchler R *et al* 2003 *Phys. Rev. Lett.* **91** 066405
[27] Donath J G, Steglich F, Bauer E D, Sarrao J L and Gegenwart P 2008 *Phys. Rev. Lett.* **100** 136401
[28] Gold C and Scheidt E-W 2008 unpublished
[29] Cox C L and Grewe N 1988 *Z. Phys.* B **71** 321
[30] Bernal O, MacLaughlin D E, Lukefahr H G and Andraka B 1995 *Phys. Rev. Lett.* **75** 2023
[31] Miranda E, Dobrosavljevic V and Kotliar G 1997 *Phys. Rev. Lett.* **78** 290
[32] Schotte K D and Schotte U 1975 *Phys. Lett.* A **55** 38
[33] Bredl C D, Steglich F and Schotte K D 1978 *Z. Phys.* B **29** 327
[34] Gribanov A *et al* 2006 *J. Phys.: Condens. Matter* **18** 9593
[35] Nieuwenhuys G J 1995 *Handbook of Magnetic Materials* ed K H J Buschow (Amsterdam: North-Holland) chapter 1, p 1
[36] Doniach S 1977 *Physica* B+C **91** 231
[37] Takke R, Niksch M, Assmus W, Lüthi B, Pott R, Schefzyk R and Wohlleben D K 1981 *J. Phys.: Condens. Matter* **44** 33
[38] Kambe S, Flouquet J, Lejey P, Hean P and de Visser A 1997 *J. Phys.: Condens. Matter* **9** 4917
[39] Küchler R, Gegenwart P, Heuser K, Scheidt E-W, Stewart G R and Steglich F 2004 *Phys. Rev. Lett.* **93** 096402
[40] Löhneysen H v 1996 *J. Phys.: Condens. Matter* **8** 9689